

## Single-Particle Diffraction and Interference at a Macroscopic Scale

Yves Couder<sup>1,\*</sup> and Emmanuel Fort<sup>2,†</sup>

<sup>1</sup>*Matières et Systèmes Complexes and Laboratoire de Physique Statistique (ENS), Université Paris 7 Denis Diderot, CNRS-UMR 7057, 4 Place Jussieu, 75 251 Paris Cedex 05, France*

<sup>2</sup>*Laboratoire Matériaux et Phénomènes Quantiques and Laboratoire de Physique du Solide (ESPCI), Université Paris 7 Denis Diderot, CNRS-UMR 7162, 4 Place Jussieu, 75 251 Paris Cedex 05, France*

(Received 13 July 2006; published 13 October 2006)

A droplet bouncing on a vertically vibrated bath can become coupled to the surface wave it generates. It thus becomes a "walker" moving at constant velocity on the interface. Here the motion of these walkers is investigated when they pass through one or two slits limiting the transverse extent of their wave. In both cases a given single walker seems randomly scattered. However, diffraction or interference patterns are recovered in the histogram of the deviations of many successive walkers. The similarities and differences of these results with those obtained with single particles at the quantum scale are discussed.

DOI: [10.1103/PhysRevLett.97.154101](https://doi.org/10.1103/PhysRevLett.97.154101)

PACS numbers: 05.45.-a, 03.65.-w, 05.65.+b, 47.55.D-

As shown recently [1], a droplet can bounce indefinitely on a vertically vibrated bath of the same fluid. Near the Faraday instability threshold [2], this bouncing becomes subharmonic and the drop emits a localized Faraday wave packet. A bifurcation occurs by which the drop becomes spontaneously self-propelled and moves on the liquid surface at constant velocity. This occurs when there is a lock-in phenomenon so that the drop falls systematically on the forward front of the wave generated by its previous bouncings [3,4]. We called "walker" the moving droplet dressed with the wave-packet it emits. A walker is a "symbiotic" structure: if the droplet disappears (by coalescence with the substrate), the wave vanishes. In reverse, if the wave is damped, the droplet stops moving. Two interacting walkers can have discrete stable orbits [3,4] demonstrating that they have both an inertia due to their mass and nonlocal interactions due to the interference of their waves.

In order to obtain a better characterization of this double particle-wave behavior of walkers we undertook the present experiments on their trajectories when they pass through apertures limiting the transverse extent of their wave. They are inspired by the well-known experiments on diffraction and interference performed at a low flux of particles. In Young's two slits configuration it was shown with photons [5], then with electrons [6–8] that interference patterns could be obtained even when only a single particle at a time was present in the system. These patterns were then observed through the accumulation of successive individual events. Such results are usually thought to be possible only in quantum physics [9].

The experiments are performed in square cells [Figs. 1(a) and 1(b)] filled with silicon oil and submitted to a vertical oscillating acceleration  $\gamma = \gamma_m \cos(2\pi f_o t)$ . Two cells of size  $70 \times 70$  mm and  $130 \times 130$  mm were used, filled with a liquid layer of thickness  $h_0 = 4$  mm. As is well-known, in this configuration, the surface of the bath can become unstable to the formation of standing waves of frequency  $f_F = f_0/2$  (and wavelength  $\lambda_F$ ). This is the parametrically forced Faraday instability [2] which occurs,

in our experiment, above a threshold  $\gamma_m^F \sim 4.5$  g. The container was carefully set horizontal and perpendicular to the vibration axis. The liquid was silicon oil with surface tension  $\sigma = 0.0209$  N/m and density  $\rho = 0.965 \times 10^3$  kg/m<sup>3</sup>. Two different oils of viscosity  $\mu_1 = 50 \times 10^{-3}$  Pa · s and  $\mu_2 = 20 \times 10^{-3}$  Pa · s were used with which walkers were optimally obtained at forcing frequencies  $f_1 = 50$  Hz and  $f_2 = 80$  Hz respectively. The measured Faraday wavelengths, ( $\lambda_F = 6.95$  and  $4.75$  mm, respectively) are in good agreement with the values computed from the dispersion relation:  $\omega^2 = \{gk + (\sigma/\rho)k^3\}$ . We used droplets of diameter  $D \sim 1$  mm, which become fast walkers with velocities of the order of a tenth of the phase velocity  $V_F^\varphi$  of the Faraday waves (with e.g.  $V_F^\varphi = 189$  mm/s for  $f_F = f_0/2 = 40$  Hz).

As sketched on Figs. 1(a) and 1(b), strips are glued to the bottom of the cell so that, above them, the depth of the liquid is reduced to  $h_1$ . In these regions the Faraday instability threshold being shifted to larger forcing amplitudes, the waves are damped and droplets either stopped or reflected. These band-shaped regions thus form opaque screens for walkers. An interval of width  $L$  between two strips forms the diffracting slit. The droplet is initially pushed into a V-shaped structure located far from the screen and formed of two segments of immersed strips. The initial direction of motion of the walker is roughly determined as it moves out of this trap.

Figure 1(a) shows a recorded droplet trajectory. While its initial motion is straight, the droplet follows a complex path as it passes through the aperture, before recovering a straight trajectory again. Figure 1(c) shows that in the slit region the wave emitted by the droplet is distorted by its interference with its own reflection on the boundaries. The deviation is clearly due to this effect. We define the far field deviation  $\alpha$  as the angle between the straight trajectories, far from the screen before and after diffraction [see Fig. 1(a)]. The first question concerns the relation between  $\alpha$  and the region of the slit the droplet has crossed. To answer this question we repeated single-particle experi-

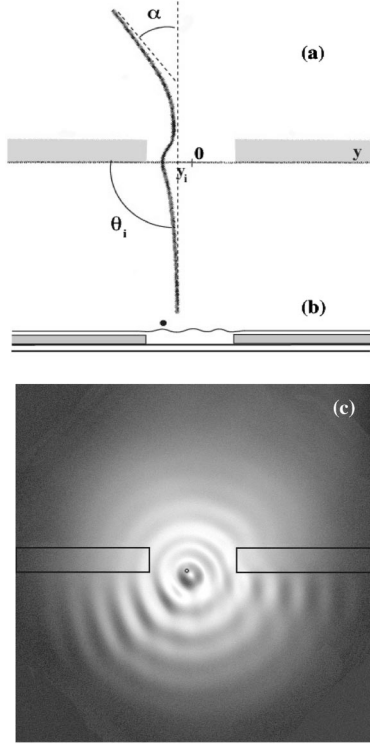


FIG. 1. (a), (b) Sketch of the central region of the experimental cell (seen from above and in a cross section along the  $y$  axis, respectively). An individual trajectory is shown in (a) and the definitions of  $\theta_i$ ,  $y_i$ , and  $\alpha$  are given. The width of the slit being  $L$ , the parameter of impact is  $Y_i = y_i/L$ . (c) A photograph of the experiment lit with diffuse light showing the wave pattern as the walker crosses the aperture. The picture was taken at a time when the trajectory, initially perpendicular to the aperture, was deflected by the interference with reflected waves.

ments, having the same walker cross the slit, with various initial motions. As shown on Fig. 1(a) each initial trajectory is defined by its incidence angle  $\theta_i$  and by its normalized impact parameter in the slit  $Y_i = y_i/L$  ( $-0.5 < Y_i < 0.5$ ) [Fig. 1(a)]. The walkers were always started far from the screen and only those impinging perpendicularly on the slit ( $\theta_i = 90^\circ$ ) were retained.

The plot  $\alpha(Y_i)$  [Fig. 2(a)] shows that there is no *simple* relation between the deviation and the parameter of impact. This is also observed on individual realizations: with apparently identical initial conditions: same droplet, same incidence angle, same  $Y_i$ , very different trajectories can be observed [Fig. 2(b)]. However, Fig. 2(a) also shows that the various values of the deviations are not observed with the same probability. We thus investigated the statistics of the deviations obtained with many independent realizations (taking care that approximately the same density of particles crosses all regions of the aperture). Figures 2(c) and 2(d) shows two histograms  $N(\alpha)$  for 125 successive events. They were obtained with the same slit (of width  $L = 14.8$  mm) with two different Faraday wavelengths:  $\lambda_F = 6.95$  mm [Fig. 2(c)] and  $\lambda_F = 4.75$  mm [Fig. 2(d)]. The central peaks have widths of the order of

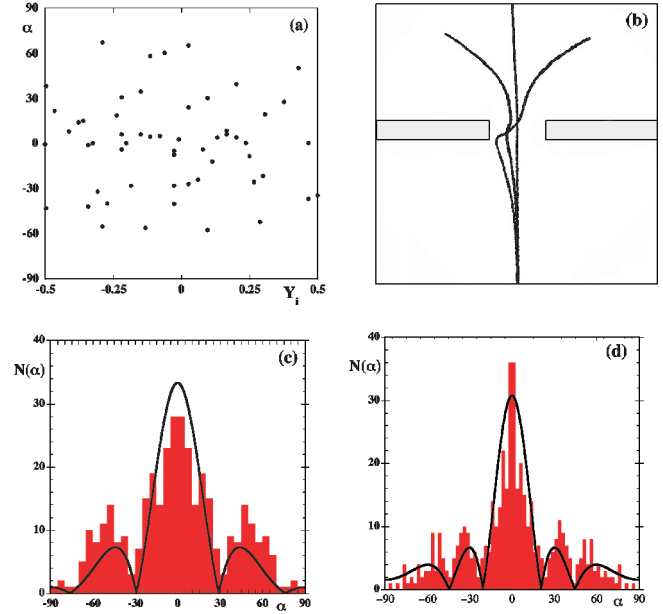


FIG. 2 (color online). (a) The measured deviations  $\alpha$  of successive individual particles as a function of the parameter of impact  $Y_i$  (with  $L/\lambda_F = 2.86$ ). (b) A superposition of three different trajectories of the same droplet passing 3 times through the slit with similar initial conditions  $\theta_i = 90^\circ$  and  $Y_i = 0.1$ . (c) Experimental histogram of the deviation  $\alpha$  as obtained with  $N_T = 125$  single walkers with  $L/\lambda_F = 2.11$  ( $L = 14.7$  mm and  $\lambda_F = 6.95$  mm). Since each trajectory has a symmetrical counterpart with respect to the axis of the aperture, the statistic was improved by taking them into account so that the distributions correspond to  $2N_T$  realizations. The curve is the fit by Eq. (1) with  $L/\lambda_F = 1.96$ . (d) Histogram obtained with  $L/\lambda_F = 3.1$  ( $L = 14.7$  mm and  $\lambda_F = 4.75$  mm). The curve is the fit by Eq. (1) with  $L/\lambda_F = 2.86$ .

$\lambda_F/L$  and large amplitude lateral lobes are clearly observed. Hence, on Figs. 2(c) and 2(d) the general shapes of the histograms are compared with the amplitude diffraction pattern of a plane wave passing through a slit:

$$f(\alpha) = A \left| \frac{\sin(\pi L \sin \alpha / \lambda_F)}{\pi L \sin \alpha / \lambda_F} \right|. \quad (1)$$

This amplitude of diffraction of a plane wave turns out to provide an approximate fit for these histograms. Hence, the particle behavior exhibits the uncertainty relation ruling the spatial confinement of a plane wave:  $\delta y (\delta \mathbf{k}_F)_y \geq 1/2$  where  $\delta y = L$  and  $\mathbf{k}_F$  is the Faraday wave vector. Let us note that diffraction here really concerns the statistical properties of trajectories of a moving source of circular waves passing through a slit, a phenomenon for which, to our knowledge, no theory exists.

These surprising results led us to go one step further and investigate if interferences with single particles could be observed. We performed Young's type of experiments using a screen with two slits. The experiment requires a fine-tuning of the forcing amplitude  $\gamma_m$  to a value very close to the Faraday threshold. The transverse extension of the

walker's wave packet is then much larger than  $d$ . Figure 3 shows the histogram of 75 such trajectories. As above we compare it to the interference amplitude pattern of a plane wave:

$$f(\alpha) = A \left| \frac{\sin(\pi L \sin\alpha/\lambda_F)}{\pi L \sin\alpha/\lambda_F} \cos(\pi d \sin\alpha/\lambda_F) \right|. \quad (2)$$

The interference fringes are clearly observed and well fitted by this expression. It can be noted that a given droplet is observed to go through one or the other of the slits. However its associated wave passes through both slits and the interference of the resulting waves is responsible for the trajectory of the walker.

Why is a droplet deviated? When a walker approaches a boundary, the shape of the surface beneath the drop results from the interference of the recent waves moving with the droplet with older waves coming back after reflection. In these conditions, due to variations of the local slope, successive jumps have different directions and lengths. The waves guide the droplet [Fig. 1(c)] and the trajectory is thus defined iteratively by a type of dynamical echolocation.

In order to evaluate the main characteristics of this remote sensing-based motion we performed numerical simulations. These simulations are an extension of the theory developed for free walkers [4,10]. We use the simplifying approximation that the vertical and horizontal motions of the droplet are decoupled. Takeoff and landing times are thus determined only by the forcing oscillations of the liquid bath. The horizontal displacement  $\delta r_n$  of the droplet between two collisions is the result of three processes. The droplet, after each takeoff, has a free parabolic motion with a constant horizontal velocity. At each

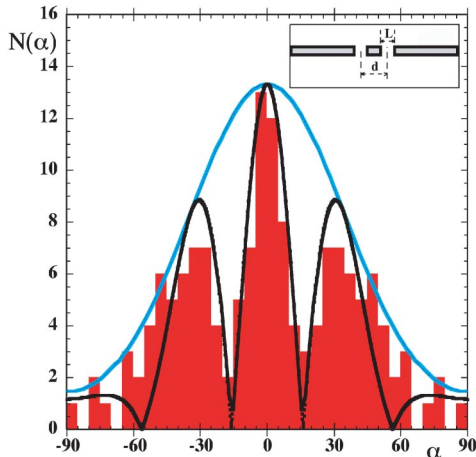


FIG. 3 (color online). Histogram for the deviation of 75 particles through two slits of width  $L = 7.6$  mm, a distance  $d = 14.3$  mm apart, the walker's wavelength being  $\lambda_F = 6.95$  mm ( $L/\lambda_F = 1.1$  and  $d/\lambda_F = 1.87$ ). The light line is the envelope due to the diffraction of a single slit while the curve in black is the optimum fit by Eq. (2) obtained for effective values  $L/\lambda_F = 0.9$  and  $d/\lambda_F = 1.7$ .

bounce, the droplet is given a momentum increment by its inelastic shock on the surface. The direction and the intensity of the kick depend on the local surface slope. During the contact time, the droplet undergoes a viscous damping of its horizontal velocity due to the shearing of the air layer between the drop and the bath. In the case of a free walker, the local slope of the interface results from the direct accumulation of the previously generated waves. With these simple hypotheses the walking bifurcation [3,4,10] is recovered.

In order to compute the effects of the surroundings on the walker's trajectory, the walls are modeled by adequately positioned secondary sources. These sources emit circular waves with a phase opposite to the wave they receive. The total wave amplitude is thus zero at the position of the secondary sources, in agreement with experimental boundary conditions. In this procedure, the influence of the scattered waves on the droplet trajectory is taken into account at each collision time, including the retardation effects due to the finite wave and droplet velocities. Experimental observations show that the wavelets produced by previous bounces of the droplet are still visible after typically 5 to 20 jumps. The calculation of the wave due to the walker includes this cumulative effect.

The trajectory of the droplet is computed iteratively,  $\delta r_n$  being at each step determined by the local slope of the interface. The new direction and amplitude of the next jump are thus the result of the interfering waves scattered by the walls or directly coming from the previous bounces at the place of collision.

The simulated droplet trajectories appear quite complex in the vicinity of the slit, in agreement with the experimental observations. This result is confirmed in Fig. 4(a) showing the deviation  $\alpha$  versus the normalized impact parameter  $Y_i$  for  $N = 250$  successive single realizations. The associated histogram of  $\alpha$  in Fig. 4(b) is similar to the amplitude diffraction of a plane wave through a slit. In spite of the simplifying assumptions the main characteristics of the experiments are recovered [11].

We have thus obtained in a classical experiment a behavior typical of wave particle duality. A discussion of the relation between these single-particle experiments and those concerning elementary particles is unavoidable. It can be first recalled that a coupling between a particle and a guiding wave is the main ingredient of an early model of quantum mechanics proposed by de Broglie [12]. Variants of this model have been developed by Bohm [13] and it was shown that single-particle interference could be obtained in this framework [14]. Our experiment turns out to implement a particular version of this type of coupling. There is, however, a huge gap between our system and the quantum world where diffraction and interference of single particles is usually observed.

The differences can be listed. Our experiment has a macroscopic scale and no relation with the Planck constant. In a walker, the wave is emitted by the particle and travels at a finite velocity on a 2D material medium. It is a

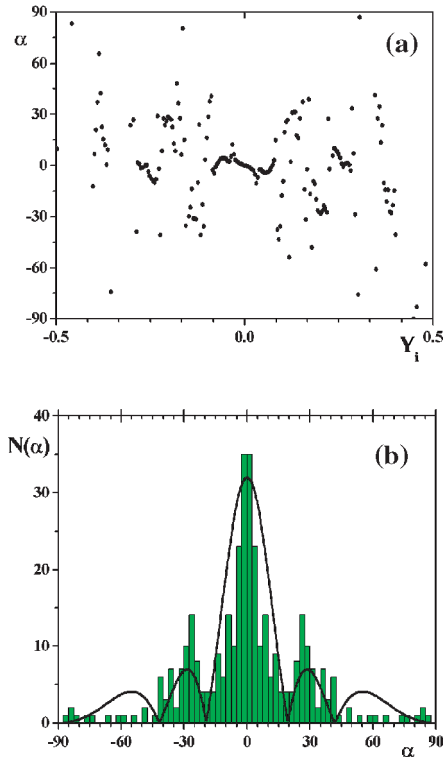


FIG. 4 (color online). Numerical simulation of the diffraction of a walker through a slit. The collision frequency is 40 Hz with an acceleration of the bath of 4.5 g. The  $\lambda_F = 5.7$  mm. The spatial and temporal attenuations of the Faraday surface waves are set at 2.5 Faraday periods and  $2.5\lambda_F$ , respectively. The iterative calculation of the slope takes into account the last 10 bounces. The walls are modeled by secondary sources periodically spaced every  $\lambda_F/2$ . Because of the limited number of the secondary sources, the deviations at very large angle are not simulated properly. (a) The deviation  $\alpha$  of individual particles as a function of the parameter of impact  $Y_i$  with  $L/\lambda_F = 3$ . (b) Histograms of the deviation  $\alpha$  as obtained with  $N = 250$  single walkers diffracted through the aperture with  $L/\lambda_F = 3$ . The curve is the fit by Eq. (1). The second lateral peaks are not visible because of the limits of simulations.

dissipative system, which is sustained by external forcing. The system is dispersive but this is masked because the wavelength is fixed by the forcing. We can measure the entire trajectory of the particles through the slits, an observation impossible in quantum mechanics [15]. Finally, because of a specific type of coupling of the particle with the wave, the probability distribution of the particles is linked with the wave amplitude (not with its intensity).

With these differences in mind we can recall the similarities. We have shown that the momentum of a walker becomes ill-defined when the transverse extent of its wave is spatially limited. This phenomenon results in a dispersion of individual deviations, together with a deterministic probability distribution of these deviations. The uncertainty principle inherent to the Fourier-transform of a wave is here responsible for a corresponding uncertainty affecting the motion of the material particle that emits the

wave. We showed in the simulation how this wavelike behavior of particle trajectories can result from the feedback of a remote sensing of the surrounding world by the waves they emit. This phenomenon gives the walking droplet a kind of nonlocality since it evolves in a medium affected by waves it emitted in the past.

We are grateful to Arezki Boudaoud, Suzie Protière, and Maurice Rossi for stimulating discussions.

\*Email address: couder@physique.ens.fr

†Email address: emmanuel.fort@espci.fr

- [1] Y. Couder, E. Fort, C. H. Gautier, and A. Boudaoud, *Phys. Rev. Lett.* **94**, 177801 (2005).
- [2] W. S. Edwards and S. Fauve, *J. Fluid Mech.* **278**, 123 (1994).
- [3] Y. Couder, S. Protière, E. Fort, and A. Boudaoud, *Nature (London)* **437**, 208 (2005).
- [4] S. Protière, A. Boudaoud, and Y. Couder, *J. Fluid Mech.* **554**, 85 (2006).
- [5] G. I. Taylor, *Proc. Cambridge Philos. Soc.* **15**, 114 (1909).
- [6] P. G. Merli, G. F. Missiroli, and G. Pozzi, *Am. J. Phys.* **44**, 306 (1976).
- [7] P. G. Missiroli, G. Pozzi, and U. Valdré, *J. Phys. E* **14**, 649 (1981).
- [8] A. Tonomura, J. Endo, T. Matsuda, T. Kawasaki, and H. Ezawa, *Am. J. Phys.* **57**, 117 (1989).
- [9] R. P. Feynman, R. B. Leighton, and M. Sands, *The Feynman Lectures on Physics* (Addison Wesley, New York, 1963), Vol. 3, Chap. 37.
- [10] In the model due to A. Boudaoud (see Ref. [4]), the forces being averaged over a period of the vertical motion, the horizontal motion is modeled by the following equation:

$$m \frac{d^2x}{dt^2} = F^b \sin\left(2\pi \frac{dx/dt}{V_\varphi}\right) = f^v \frac{dx}{dt}.$$

The first term on the right is the effective force due to the bouncing on an inclined surface. It is proportional to  $\gamma_m$  and to the slope of the surface waves. The actual tilt of the surface at the time of collision results from the difference in propagation of the drop and the wave since the previous collision. The argument of the sine corresponds to this phase shift. The second term stands for the viscous damping due to the shearing of the air layer between the drop and the bath during the contact.

- [11] The fact that the elementary displacement of the drop is related to the slope of the surface (and thus to the wave amplitude) appears to be responsible for the amplitude related diffraction or interference patterns.
- [12] L. de Broglie, *Ondes et mouvements* (Gautier Villars, Paris, 1926).
- [13] D. Bohm, *Phys. Rev.* **85**, 166 (1952).
- [14] C. Philippidis, C. Dewdney, and B. J. Hiley, *Nuovo Cimento B* **52**, 15 (1979).
- [15] It can be noted however, that it would not be possible to observe the phenomenon by any means at its scale. For instance, the use of a floater to measure the waves would destroy the diffraction or interference pattern.